Heliyon 8 (2022) e08691

Contents lists available at ScienceDirect

Heliyon

journal homepage: www.cell.com/heliyon

Research article

Total body proton and heavy-ion irradiation causes cellular senescence and promotes pro-osteoclastogenic activity in mouse bone marrow

Kamendra Kumar [a], Kamal Datta [a], Albert J. Fornace Jr. [a,b], Shubhankar Suman [a,*]

[a] Department of Oncology, Lombardi Comprehensive Cancer Center, Georgetown University Medical Center, Washington, DC 20057, USA
[b] Department of Biochemistry and Molecular & Cellular Biology, Georgetown University Medical Center, Washington, DC 20057, USA

ARTICLE INFO

Keywords:
High-LET radiation
Senescence
Osteoclastogenesis
Bone marrow
RANK-ligand
Total body irradiation

ABSTRACT

Low-LET photon radiation-induced persistent alterations in bone marrow (BM) cells are well documented in total-body irradiated (TBI) rodents and also among radiotherapy patients. However, the late effects of protons and high-LET heavy-ion radiation on BM cells and its implications in osteoclastogenesis are not fully understood. Therefore, C57BL6/J female mice (8 weeks; n = 10/group) were irradiated to sham, and 1 Gy of the proton (0.22 keV/μm), or high-LET ^{56}Fe-ions (148 keV/μm) and at 60 d post-exposure, mice were sacrificed and femur sections were obtained for histological, cellular and molecular analysis. Cell proliferation (PCNA), cell death (active caspase-3), senescence (p16), osteoclast (RANK), osteoblast (OPG), osteoblast progenitor (c-Kit), and osteoclastogenesis-associated secretory factors (like RANKL) were assessed using immunostaining. While no change in cell proliferation and apoptosis between control and irradiated groups was noted, the number of BM megakaryocytes was significantly reduced in irradiated mice at 60 d post-exposure. A remarkable increase in p16 positive cells indicated a persistent increase in cell senescence, whereas increased RANKL/OPG ratio, reductions in the number of osteoblast progenitor cells, and osteocalcin provided clear evidence that exposure to both proton and ^{56}Fe-ions promotes pro-osteoclastogenic activity in BM. Among irradiated groups, ^{56}Fe-induced alterations in the BM cellularity and osteoclastogenesis were significantly greater than the protons that demonstrated a radiation quality-dependent effect. This study has implications in understanding the role of IR-induced late changes in the BM cells and its involvement in bone degeneration among deep-space astronauts, and also in patients undergoing proton or heavy-ion radiotherapy.

1. Introduction

Bone marrow (BM) is a radiosensitive tissue, and therefore, astronauts undertaking deep space missions are at a greater risk of developing space radiation-induced BM alterations that could adversely affect their overall health (Almeida-Porada et al., 2018). Solar particle events (SPEs) and galactic cosmic radiation (GCR) are two main sources of ionizing radiation (IR) in the outer space (Furukawa et al., 2020), where protons are the major constituent of both the SPEs (~90%) and the GCR (~87 %) (Muralidharan et al., 2015; Norbury et al., 2016). In addition to highly abundant protons, high-linear energy transfer (LET) heavy ions constitute only 1–2 % of total GCR but contribute up to 89 % of the total equivalent dose due to its densely ionizing characteristics (Walker et al., 2013). Therefore, exposure to either highly abundant protons or densely ionizing heavy ions is predicted to adversely impact BM cells and their function in astronauts. However, the differential impact of protons and heavy ions on BM cells and its implications in IR-induced BM damage associated pathologies are need to be better defined.

Previous studies using radiotherapy patients and *in-vivo* total-body irradiated (TBI) animal models have shown long-term adverse changes in the BM compartment after low and high- LET IR exposure (Liu et al., 2019; Restier-Verlet et al., 2021; Suman et al., 2012; Chang et al., 2017b; Datta et al., 2012). IR-induced late BM alterations are often marked by elevated oxidative stress, DNA damage, senescence, decreased cellularity, and altered cellular differentiation (Wang et al., 2017; Yu et al., 2010; Schönmeyr et al., 2008; Manolagas and Jilka, 1995; Mauch et al., 1995; Green et al., 2012; Greenberger and Epperly, 2009; FitzGerald et al., 1986; Akeem et al., 2019; Chang et al., 2017a; Amsel and Dell, 1971). Bone-forming osteoblast (OB) and bone-resorbing osteoclast (OC) cells originate from BM-mesenchymal (BM-MSCs) and hematopoietic stem cells (HSCs), respectively (Boyle et al., 2003; Teitelbaum, 2000), and alterations in the number, and differentiation of BM stem cells have

* Corresponding author.
E-mail address: ss2286@georgetown.edu (S. Suman).

https://doi.org/10.1016/j.heliyon.2021.e08691
Received 18 October 2021; Received in revised form 1 December 2021; Accepted 27 December 2021

been observed during low-LET IR-induced premature aging (Richardson, 2009). Therefore, IR-induced BM damage could potentially result in depletion of OBs and activation of OC might trigger osteoclastogenesis and subsequent bone loss (Donaubauer et al., 2020). However, osteoclastogenic effects of proton and heavy-ion radiation in BM compartment is not well understood. Based on differences in the biophysical characteristics and relative biological effectiveness (RBE) of proton and heavy-ion radiation (Magrin et al., 2015; Kennedy, 2014; Choi and Kang, 2012), we hypothesized that IR-induced pro-osteoclastogenic changes in the BM might depend on radiation quality. The term "radiation quality" represents the ionization-associated biological damage after various types of IR, which primarily depends on the LET. Exposure to high-LET high radiation quality IR, such as ^{56}Fe-ion usually causes dense ionization and more biological damage relative to protons.

Osteoclastogenesis requires progenitor stem cell differentiation to pre-OC, and its activation to bone resorbing OC. The receptor activator of NF-κB ligand (RANKL) and receptor activator of NF-κB (RANK) signaling is considered the major driver of osteoclastogenesis, while osteoprotegerin (OPG) prevents osteoclastogenesis by binding to RANKL and preventing it from binding to RANK (Boyce & Xing, 2007, 2008). Thus, higher RANKL/OPG ratio denotes pro-osteoclastogenic activity (Boyce and Xing, 2008). TBI at <2 Gy dose has been reported to promote osteoclastogenesis, marked by increased gene expression of *Rankl* and higher *Rankl/Opg* ratio (Alwood et al., 2015). Additionally, IR-induced loss of osteogenic activity in the BM is also possible through decreased number of megakaryocytes (MKs) and osteocalcin positive cells in the marrow (Schönmeyr et al., 2008; Shao et al., 2014), where MKs have been shown to stimulate OB proliferation and simultaneously inhibiting OC through secretion of anti-resorptive factors (Kacena et al., 2006; Lee et al., 2020), and a higher number of osteocalcin positive cells in the BM coincides with higher osteogenic activity (Eghbali-Fatourechi et al., 2005).

In this study we investigated the late molecular and cellular consequences of proton and heavy ion (^{56}Fe) radiation exposure on TBI mouse BM and report that proton and ^{56}Fe radiation led to increased BM cell senescence and accumulations of osteoclastogenic markers while reducing the number of OBs, MKs and OB progenitor cells in a radiation quality dependent manner. This study provides an intriguing insight into the differential effects of proton and heavy ion (^{56}Fe) induced pro-osteoclastogenic changes in the BM.

2. Results

2.1. Reductions in megakaryocytes count and increased number of senescent cells in mouse bone marrow after proton and ^{56}Fe-ion exposure

Hematoxylin and eosin stained histopathology of BM exhibited a significant decrease in the number of megakaryocytes after proton and ^{56}Fe-ion exposure as compared to their age matched controls (Figure 1B-C). Further, number of megakaryocytes in the ^{56}Fe-ion irradiated mice was significantly reduced as compared to the proton irradiated group (Figure 1C). To examine the possible role of protons and ^{56}Fe-ion exposure on the BM proliferation, apoptosis, and senescence, we performed immunohistochemistry to measure their level of expression in two months post-irradiation bone marrow tissues (Figure 2). Results showed no remarkable alterations in the number of PCNA positive proliferative cells (Figure 2A-B) and active-caspase-3 positive apoptotic cells (Figure 2A and C) in the proton and ^{56}Fe-ion irradiated samples with respect to age-matched controls. However, a significant increase in the p16 positive senescent cells (Figure 2A and D) was observed in the BM of proton and ^{56}Fe-ion irradiated mice relative to controls. In addition, the number of senescent cells, as determined by p16 staining, were significantly more in ^{56}Fe-ion irradiated mice relative to age matched proton irradiated mice (Figure 2D), suggesting a radiation quality dependent effects on bone marrow senescence.

2.2. Proton and ^{56}Fe-ion induced pro-osteoclastogenic changes in mouse bone marrow

Immunoreactivity of RANK and RANKL was significantly higher in the bone marrow sections of both proton and ^{56}Fe-ion irradiated mice with respect to the controls (Figure 3A), However, OPG expression was decreased in both proton and ^{56}Fe-ion groups (Figure 3A). Quantitation

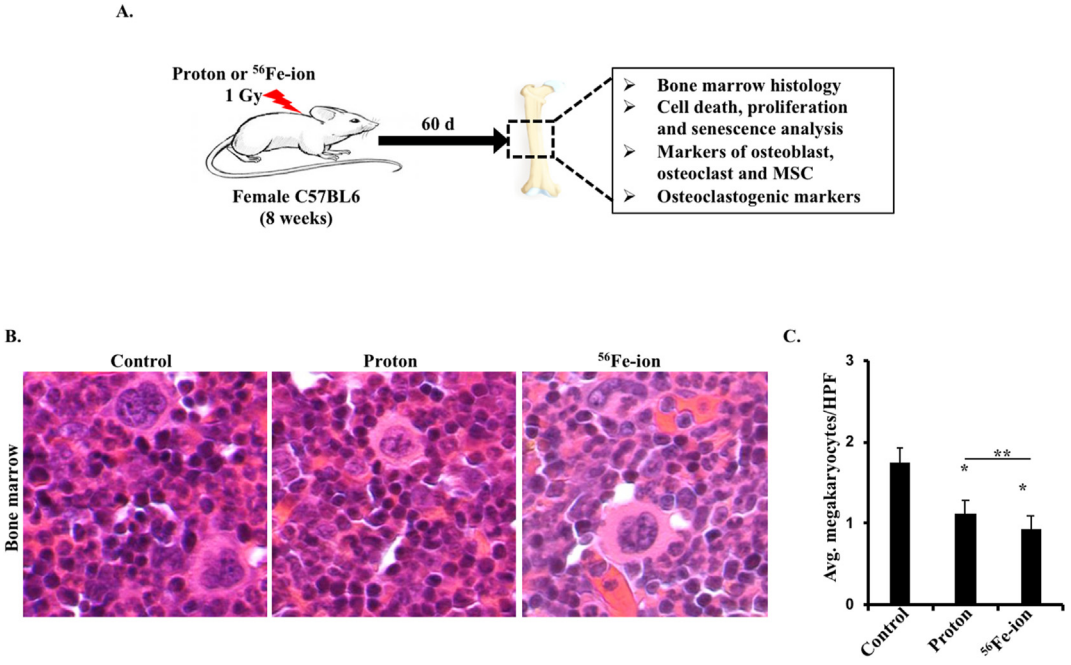

Figure 1. Histological analysis of hematoxylin and eosin (H&E) stained bone-marrow and compact bone sections from control, proton, and ^{56}Fe-ion exposed mice after 2 months post-exposure (n = 6 mice/group). A) Schematic overview of experimental plan. B) Representative photomicrographs (magnification 400x) showing reductions in bone marrow megakaryocyte count and reductions in bone osteocyte count after 1 Gy of proton and ^{56}Fe-ion exposure. C) Quantification of megakaryocytes in bone-marrow. D) Quantification of osteocytes in bone. Each bar represents mean ± SEM values obtained from 10 to 12 high power field (HPF) from n = 5 mice/group. * denotes $p < 0.05$ compared to the control group and ** denotes $p < 0.05$ between irradiated groups.

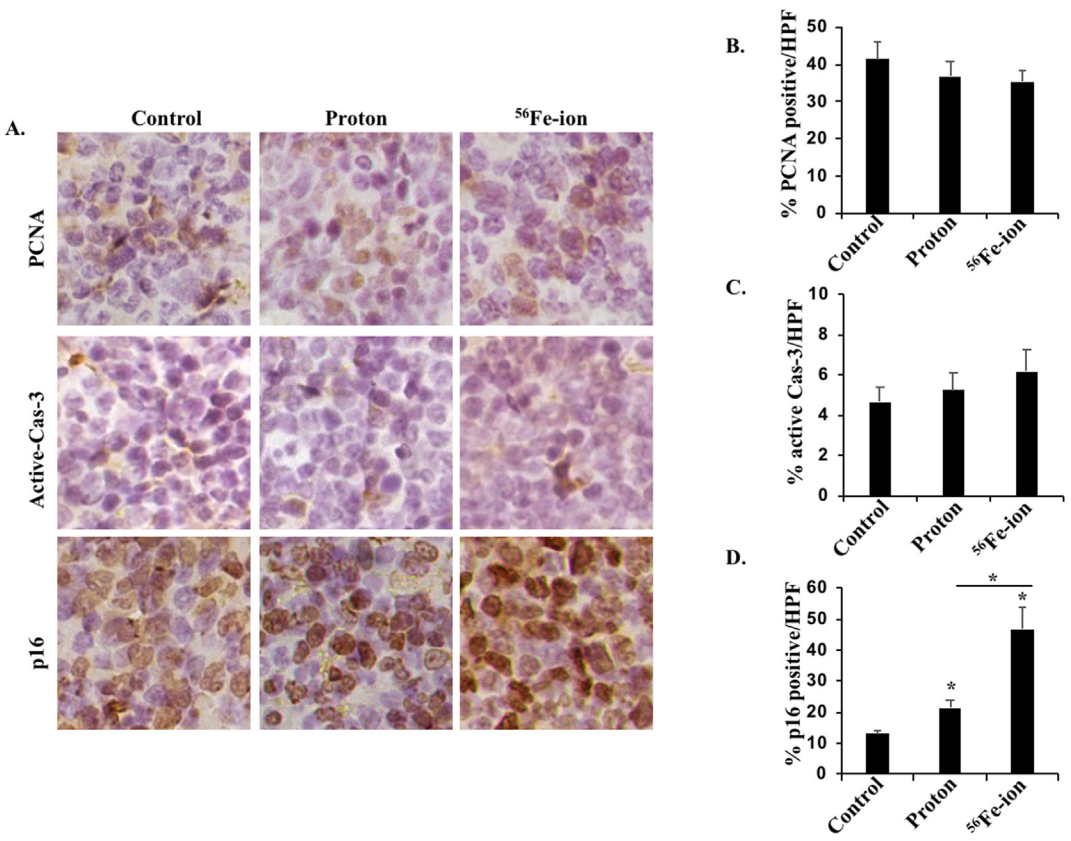

Figure 2. Effect of proton and ^{56}Fe-ion exposure on cell proliferation, cell-death and senescence in mouse bone marrow at 2 months post-exposure. A) Representative photomicrographs (magnification 400x) showing immunohistochemical staining of PCNA (proliferation), active caspase-3 (cell death), and p16 (senescence) after 1 Gy of proton and ^{56}Fe-ion exposure. B) Quantification of PCNA positive cells. C) quantification of active caspase-3 positive cells, and D) quantification of p16 positive cells. Each bar represents mean ± SEM values obtained from 10 HPF (high power field) with n = 5 mice/group and * denotes statistically significant change ($p < 0.05$) relative to the control group.

of RANKL/OPG ratio indicated a significant increase in osteoclastogenic activity in the BM of both proton and ^{56}Fe-ion irradiated mice (Figure 3B). Further, an increase in RANKL/OPG and osteoclast/osteoblast ratio indicated activation of osteoclastogenesis in BM of the proton and ^{56}Fe-ion irradiated mice. In addition, the osteoclast/osteoblast ratio was also significantly different in proton and ^{56}Fe-ion group, suggesting more pronounced effects of ^{56}Fe-ion exposure (Figure 3C).

2.3. Reduced osteoblast progenitors and osteocalcin expression in mouse bone marrow after proton and ^{56}Fe-ion exposure

In order to understand the effect of proton and ^{56}Fe-ions on the bone anabolic process, we performed immunofluorescence staining of BM sections to analyze the number and expression of osteoblast progenitor and bone anabolic factor osteocalcin, respectively (Figure 4). We found reduced expression of osteocalcin in both proton and ^{56}Fe-ion groups, relative to controls (Figure 4B). Moreover, a statistically significant reduction was observed in the ^{56}Fe-ion group relative to protons that indicates a radiation quality dependent effect on osteocalcin expression. Further, the percentage of c-Kit expressing osteoblast progenitor was also decreased in both proton and ^{56}Fe-ion groups, relative to sham (Figure 4C). Reductions in the number and expression of osteoblast progenitor and osteocalcin clearly indicates dampening of bone anabolic signaling in the BM compartment after IR exposure.

3. Discussion

IR exposure has been demonstrated to cause persistent cellular senescence in many tissue types, including the BM cells (Chang et al., 2015, 2017b). In this study, using proton and ^{56}Fe -ion irradiated mice we demonstrated a significant increase in senescence, and no appreciable change in cell proliferation and cell death in BM cells. Further, we observed the decrease in MKs, osteoblast progenitors, OBs, osteocalcin, OPG expression and increased pro-osteoclastogenic RANKL, and RANKL/OPG ratio in the BM cells, which indicates a pro-osteoclastgenic and an anti-oesteogenic response to both proton and ^{56}Fe-ion exposure. Notably, a radiation quality dependent increase in pro-osteoclastogenic changes in the BM was evident as ^{56}Fe-induced alterations were significantly greater than the proton.

Increased accumulations of p16 positive senescent cells in BM have been observed long-term after low-LET IR exposure (Nguyen et al., 2018; Singh et al., 2018; Geiger, 2014), whereas, here using TBI proton and ^{56}Fe-ion exposure we demonstrated LET-dependent increase in BM cell senescence after proton and ^{56}Fe-ion exposure. In concurrence, *in vivo* study using low-LET and ^{56}Fe-ion exposures have also demonstrated increased G1 arrest in BM cells (Rithidech et al., 2008; Alessio et al., 2015). While BM-HSCs and BM-MSCs differ in their radiosensitivity, both have been shown to undergo premature senescence in response to IR-stress (Cmielova et al., 2012) that might affect number and functions of their respective differentiated progenies. Since OBs originate from BM-MSCs (Zhao et al., 2014; Dominici et al., 2009; Xiao et al., 2017; Macaulay et al., 2013) and MKs can induce osteoblastogenesis via secreting osteogenic factors (Kelm et al., 1992; Breton-Gorius et al., 1992; Chenu and Delmas, 1992), therefore, reductions in the number of MKs and OBs might reflects IR-induced persistent suppression of stem cell differentiation to osteogenic OB cells. Additionally, decreased expression of osteogenic factor osteocalcin, after proton and ^{56}Fe-ion exposure also demonstrates an anti-osteogenic effect, that has also been observed earlier after low-LET irradiation (Schönmeyr et al., 2008).

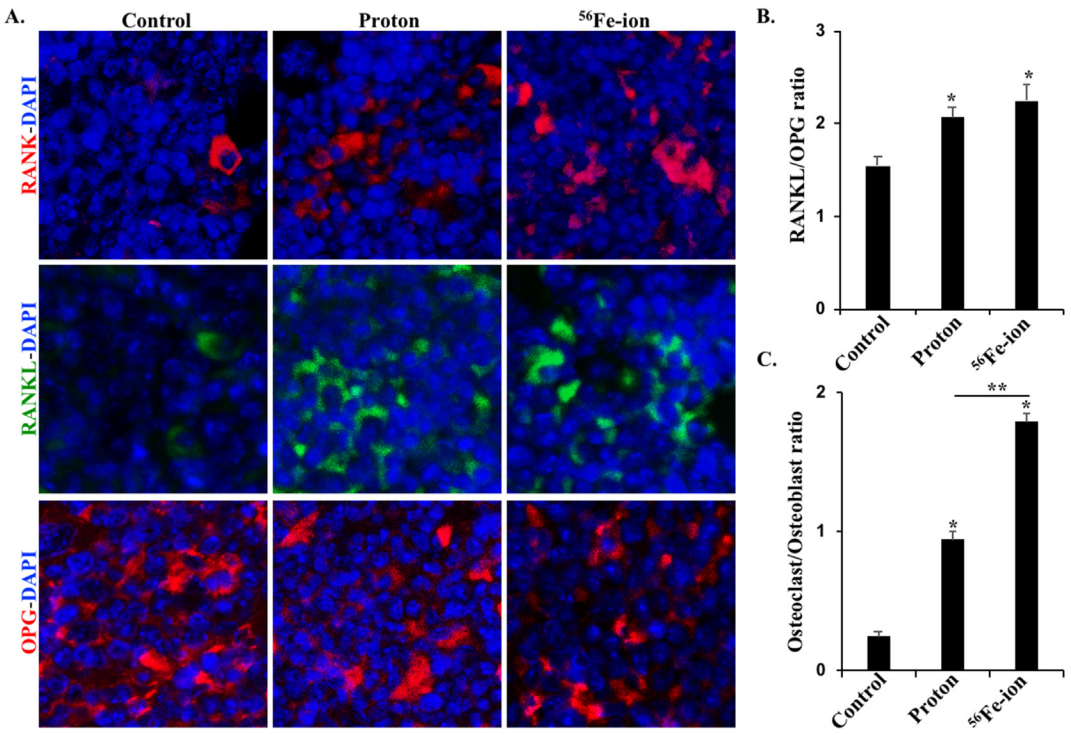

Figure 3. Analysis of osteoclastogenic markers in the bone marrow cells after proton and ^{56}Fe exposure. A) Representative immunofluorescence images (magnification 400x) depicting RANK (osteoclast marker), RANKL (osteoclastogenesis marker) and OPG (osteoblast marker) expressing cells. B) Quantification of RANKL/OPG ratio from immuno-stained sections. C) Quantification of osteoclast/osteoblast ratio from immuno-stained sections. Each bar represents mean ± SEM values from 10 to 12 HPF with n = 5 mice/group. * denotes $p < 0.05$ compared to the control group and ** denotes $p < 0.05$ between irradiated groups.

Findings of this study also corroborates with previous studies showing increased osteoclastogenesis after total body IR exposure at <2 Gy dose (Alwood et al., 2015; Yang et al., 2012; Zhang et al., 2017) and also confirms earlier radiation quality dependent increase in *Rankl* expression in the BM (Alwood et al., 2015). Additionally, anti-osteoclastogic factor OPG is also reduced after IR exposure (Sharaf-Eldin et al., 2016), hence would likely not prevent from IR-induced RANKL-mediated osteoclastogenesis (Rana et al., 2012). IR-induced osteoclastogenic activity in BM might also contribute in bone loss (Su et al., 2018; Grigor'ev et al., 2013; Bandstra et al., 2009; Willey et al., 2011b), which is consistent with significant loss of bone volume and increased osteoclast activity after clinically relevant doses of γ, protons, and ^{12}C-ions radiation (Hamilton et al., 2006; Willey et al., 2011b). Moreover, degenerative changes in the bone has also been reported at spaceflight-relevant radiation doses (Willey et al., 2011a). While this study demonstrates increased pro-osteoclastogenic activity using space radiation, other studies showed similar effects using additional space flight related factors such as microgravity (Stavnichuk et al., 2020). Therefore, further studies combining microgravity and space radiation would be important to assess BM-associated health risk of deep space missions on astronauts' health.

Moreover, radiation quality-dependent accelerated-senescence in BM cells, likely involve the acquisition of the senescence associated secretory phenotype (SASP) and pro-osteoclastogenic secretion from these cells plausibly results in persistent osteoclastogenesis (Wang et al., 2021; Gorissen et al., 2018), as observed in aged mice (Cao et al., 2003, 2005; Shahnazari et al., 2012). The role of SASP-associated overexpression of RANKL in osteoclastogenesis is well established and emerging reports on IR-induced premature aging have also demonstrated the role of RANKL in osteoclastogenesis (Pignolo et al., 2021). While SASP factors like RANKL, could originate from various tissue types after TBI, however, the RANKL expressed from BM cells after TBI might be the major contributor to the osteoclastogenesis. Based upon these findings, it is conceivable that deciphering underlying signaling mechanism of IR-induced persistent accumulations of senescent cells and SASP-associated RANKL overexpression are important, and suggest that known anti-senescence/aging therapies might provide significant protection against space radiation-induced degenerative changes in the BM and bone.

4. Materials and methods

4.1. Animal care and irradiations

Female C57BL6/J mice (7 weeks) were shipped to Brookhaven National Laboratory (BNL) animal facility and acclimated for 1 week followed by total-body sham, proton (LET: 0.22 keV/micron) or ^{56}Fe-ion (LET: 148 keV/micron) exposure at the age of 8 weeks, as described previously (Datta et al., 2012). The next day following irradiation, all animals were shipped to Georgetown University (GU) animal facility via an approved same-day animal courier service. All animals were group-housed in well-ventilated cages with *ad libitum* access to food and water. Animal maintenance, irradiation, and all experimental procedures in this study were performed in accordance with our approved IACUC protocol at both GU and BNL. The GU-IACUC protocol # 07–009 (renumbered as # 2016-1129), was initially approved on 31st Jan 2007, renewed every three years, and active until 18th Jan-2022) and the BNL-IACUC protocol # 345, was initially approved on 8th Feb-2007 and renewed annually, active until 6th Feb-2022).

4.2. Sample collection and histological assessments

A schematic summary of sample collection and the experimental plan is provided in Figure 1A. At 60 d post-exposure, mice were sacrificed using carbon dioxide inhalation, and femurs were surgically dissected and fixed overnight in 10% buffered formalin, followed by decalcification, and paraffin embedding. Finally, 5–7 μm thick transverse sections from the central tubular region (diaphysis) of the femur were obtained for Hematoxylin and Eosin (H&E) and immunostaining. Digitized images

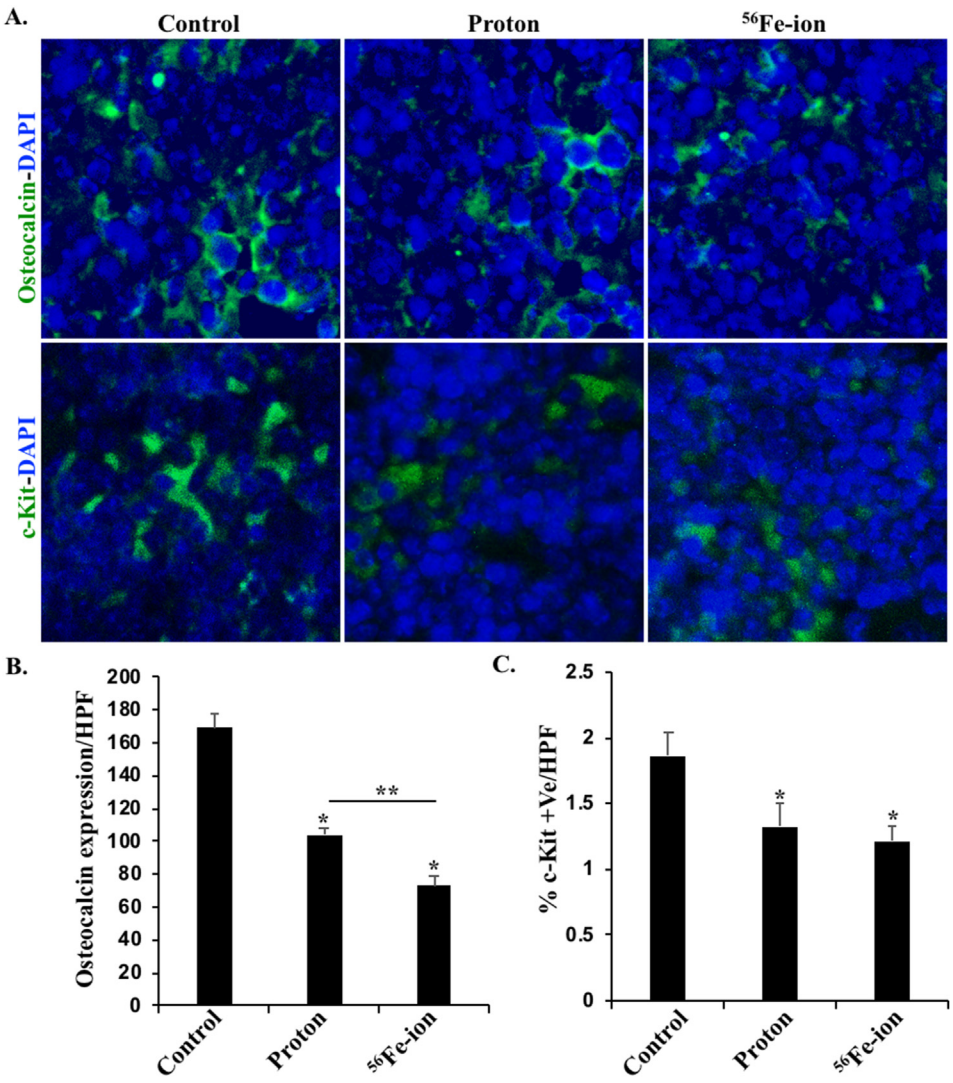

Figure 4. Analysis of osteogenic markers in the bone marrow cells after proton and ^{56}Fe exposure. A) Representative immunofluorescence images (magnification 400x) depicting Osteocalcin (osteogenesis marker) and c-Kit (osteoblast progenitor marker). B) Quantification of Osteocalcin expressing cells/HPF. C) Quantification of c-Kit positive cells/HPF. Each bar represents mean ± SEM values from 10 to 12 HPF with n = 5 mice/group. * denotes $p < 0.05$ compared to the control group and ** denotes $p < 0.05$ between irradiated groups.

of the H&E stained BM sections were obtained using bright field microscopy (Olympus BX63) followed by megakaryocytes quantitation.

4.3. In-situ immunostaining

Formalin-fixed paraffin-embedded (FFPE) femur sections were processed for immunostaining either using immunohistochemistry (IHC) or immunofluorescence (IF), as described previously (Datta et al., 2014). Briefly, tissue sections were deparaffinized, rehydrated and antigen-retrieval was performed using citrate buffer pH 6.0 (Electron Microscopy Sciences, Hatfield, PA), as per manufactures recommendation. After blocking for non-specific protein binding and endogenous peroxidase, tissue sections were incubated overnight with primary antibodies: anti-PCNA (1:200 dilution, sc-7907; Santa Cruz, Dallas, TX); anti-p16 (1:1000 dilution, MAS-17142; Invitrogen, Carlsbad, CA); anti-active caspase-3 (1:500 dilution, 2305-PC-100; Trevigen, Gaithersburg, MD); anti-RANK (1:200 dilution; ab13918; Abcam, Cambridge, UK); anti-sRANKL (1:50 dilution; MA1-20347; Invitrogen, Carlsbad, CA); Anti-osteocalcin (1:400 dilution; ab13918, Abcam); anti-cKit (1:150 dilution, ab231780; Abcam); and anti-OPG (1:500 dilution, NB100–56505SS; Novus Biologicals, Littleton, CO) at 4 °C. After multiple washing steps, IHC signal was detected using Mouse and Rabbit Specific HRP/DAB IHC Detection Kit (ab236466, Abcam, Cambridge, UK) followed by counterstaining using Mayer's Hematoxylin (26043-06, Electron Microscopy Sciences, Hatfield, PA), and finally stained sections were dehydrated and permanently mounted using Permount mounting medium (SP15-100, Fisher Scientific, Waltham, MA). In case of IF, following primary antibody incubation, slides were washed with ice-cold PBS and incubated with appropriate secondary antibodies: Donkey anti-mouse (1:200, Alexa Fluor 594, Molecular Probe, Eugene, OR) Donkey anti-rabbit (1:200, Alexa Fluor 488, Molecular Probe, Eugene, OR) and Goat anti-mouse (1:200, Alexa Fluor 488, Molecular Probe, Eugene, OR) followed by nuclear counterstaining using the aqueous mounting medium with DAPI (17989-20; Electron Microscopy Sciences, Hatfield, PA). In order to maintain reproducibility, all immunostaining was conducted with appropriate controls.

4.4. Image analysis and quantification

Bright-field and fluorescence images from immunostained slides of control, proton, and ^{56}Fe-ion groups were captured at the same setting using cellSense imaging software, respectively. Finally, all images were saved as a TIFF file and 10 or more digitalized images from each group were used for either signal intensity or the number of positive nuclei/high per field (HPF) using Fiji (Image-J) software package (Schindelin et al., 2012).

4.5. Statistical analysis

All quantitative data were expressed as mean ± standard error of the mean (SEM). Statistical differences between irradiated vs. control and

between irradiated groups (proton vs. ^{56}Fe) were analyzed using student paired sample t-test. Data analysis was performed using GraphPad Prism 6.0 for Mac (GraphPad Software, La Jolla, CA).

Declarations

Author contribution statement

Kamendra Kumar: Conceived and designed the experiments; Performed the experiments; Analyzed and interpreted the data; Wrote the paper.

Kamal Datta, Albert J Fornace Jr.: Contributed reagents, materials, analysis tools or data; Wrote the paper.

Shubhankar Suman: Conceived and designed the experiments; Analyzed and interpreted the data; Contributed reagents, materials, analysis tools or data; Wrote the paper.

Funding statement

This work was supported by National Aeronautics and Space Administration (NASA) grant NNX09AU95G and institutional funds.

Data availability statement

No data was used for the research described in the article.

Declaration of interests statement

The authors declare no conflict of interest.

Additional information

No additional information is available for this paper.

Acknowledgements

We highly appreciate help and support from Dr. Peter Guida, Dr. Adam Rusek, and all the support staff at NASA Space Radiation Laboratory (NSRL). We also acknowledge Ms. Ake Pelagie's help with animal colony maintenance.

References

Akeem, S., Lukman, O., Eltahir, K., Fatai, O., Abiola, B., Khadijat, O., 2019. Bone marrow and peripheral blood cells toxicity of a single 2.0 Gy Cobalt^{60} ionizing radiation: an animal model. Ethiop J. Health Sci. 29, 195–202.

Alessio, N., Del Gaudio, S., Capasso, S., Di Bernardo, G., Cappabianca, S., Cipollaro, M., Peluso, G., Galderisi, U., 2015. Low dose radiation induced senescence of human mesenchymal stromal cells and impaired the autophagy process. Oncotarget 6, 8155–8166.

Almeida-Porada, G., Rodman, C., Kuhlman, B., Brudvik, E., Moon, J., George, S., Guida, P., Sajuthi, S.P., Langefeld, C.D., Walker, S.J., Wilson, P.F., Porada, C.D., 2018. Exposure of the bone marrow microenvironment to simulated solar and galactic cosmic radiation induces biological bystander effects on human hematopoiesis. Stem Cell. Dev. 27, 1237–1256.

Alwood, J.S., Shahnazari, M., Chicana, B., Schreurs, A.S., Kumar, A., Bartolini, A., Shirazi-Fard, Y., Globus, R.K., 2015. Ionizing radiation stimulates expression of pro-osteoclastogenic genes in marrow and skeletal tissue. J. Interferon Cytokine Res. 35, 480–487.

Amsel, S., Dell, E.S., 1971. The radiosensitivity of the bone-forming process of heterotopically-grafted rat bone-marrow. Int. J. Radiat. Biol. Relat. Stud. Phys. Chem. Med. 20, 119–127.

Bandstra, E.R., Thompson, R.W., Nelson, G.A., Willey, J.S., Judex, S., Cairns, M.A., Benton, E.R., Vazquez, M.E., Carson, J.A., Bateman, T.A., 2009. Musculoskeletal changes in mice from 20-50 cGy of simulated galactic cosmic rays. Radiat. Res. 172, 21–29.

Boyce, B.F., Xing, L., 2007. The RANKL/RANK/OPG pathway. Curr. Osteoporos. Rep. 5, 98–104.

Boyce, B.F., Xing, L., 2008. Functions of RANKL/RANK/OPG in bone modeling and remodeling. Arch. Biochem. Biophys. 473, 139–146.

Boyle, W.J., Simonet, W.S., Lacey, D.L., 2003. Osteoclast differentiation and activation. Nature 423, 337–342.

Breton-Gorius, J., Clezardin, P., Guichard, J., Debili, N., Malaval, L., Vainchenker, W., Cramer, E.M., Delmas, P.D., 1992. Localization of platelet osteonectin at the internal face of the alpha-granule membranes in platelets and megakaryocytes. Blood 79, 936–941.

Cao, J., Venton, L., Sakata, T., Halloran, B.P., 2003. Expression of RANKL and OPG correlates with age-related bone loss in male C57BL/6 mice. J. Bone Miner. Res. 18, 270–277.

Cao, J.J., Wronski, T.J., Iwaniec, U., Phleger, L., Kurimoto, P., Boudignon, B., Halloran, B.P., 2005. Aging increases stromal/osteoblastic cell-induced osteoclastogenesis and alters the osteoclast precursor pool in the mouse. J. Bone Miner. Res. 20, 1659–1668.

Chang, J., Feng, W., Wang, Y., Allen, A.R., Turner, J., Stewart, B., Raber, J., Hauer-Jensen, M., Zhou, D., Shao, L., 2017a. ^{28}Si total body irradiation injures bone marrow hematopoietic stem cells via induction of cellular apoptosis. Life Sci. Space Res. 13, 39–44.

Chang, J., Feng, W., Wang, Y., Luo, Y., Allen, A.R., Koturbash, I., Turner, J., Stewart, B., Raber, J., Hauer-Jensen, M., Zhou, D., Shao, L., 2015. Whole-body proton irradiation causes long-term damage to hematopoietic stem cells in mice. Radiat. Res. 183, 240–248.

Chang, J., Wang, Y., Pathak, R., Sridharan, V., Jones, T., Mao, X.W., Nelson, G., Boerma, M., Hauer-Jensen, M., Zhou, D., Shao, L., 2017b. Whole body proton irradiation causes acute damage to bone marrow hematopoietic progenitor and stem cells in mice. Int. J. Radiat. Biol. 93, 1312–1320.

Chenu, C., Delmas, P.D., 1992. Platelets contribute to circulating levels of bone sialoprotein in human. J. Bone Miner. Res. 7, 47–54.

Choi, J., Kang, J.O., 2012. Basics of particle therapy II: relative biological effectiveness. Radiat. Oncol. J 30, 1–13.

Cmielova, J., Havelek, R., Soukup, T., Jiroutová, A., Visek, B., Suchánek, J., Vavrova, J., Mokry, J., Muthna, D., Bruckova, L., Filip, S., English, D., Rezacova, M., 2012. Gamma radiation induces senescence in human adult mesenchymal stem cells from bone marrow and periodontal ligaments. Int. J. Radiat. Biol. 88, 393–404.

Datta, K., Suman, S., Fornace, A.J., 2014. Radiation persistently promoted oxidative stress, activated mTOR via PI3K/Akt, and downregulated autophagy pathway in mouse intestine. Int. J. Biochem. Cell Biol. 57, 167–176.

Datta, K., Suman, S., Trani, D., Doiron, K., Rotolo, J.A., Kallakury, B.V., Kolesnick, R., Cole, M.F., Fornace, A.J., 2012. Accelerated hematopoietic toxicity by high energy (56)Fe radiation. Int. J. Radiat. Biol. 88, 213–222.

Dominici, M., Rasini, V., Bussolari, R., Chen, X., Hofmann, T.J., Spano, C., Bernabei, D., Veronesi, E., Bertoni, F., Paolucci, P., Conte, P., Horwitz, E.M., 2009. Restoration and reversible expansion of the osteoblastic hematopoietic stem cell niche after marrow radioablation. Blood 114, 2333–2343.

Donaubauer, A.J., Deloch, L., Becker, I., Fietkau, R., Frey, B., Gaipl, U.S., 2020. The influence of radiation on bone and bone cells-differential effects on osteoclasts and osteoblasts. Int. J. Mol. Sci. 21.

Eghbali-Fatourechi, G.Z., Lamsam, J., Fraser, D., Nagel, D., Riggs, B.L., Khosla, S., 2005. Circulating osteoblast-lineage cells in humans. N. Engl. J. Med. 352, 1959–1966.

FitzGerald, T.J., McKenna, M., Rothstein, L., Daugherty, C., Kase, K., Greenberger, J.S., 1986. Radiosensitivity of human bone marrow granulocyte-macrophage progenitor cells and stromal colony-forming cells: effect of dose rate. Radiat. Res. 107, 205–215.

Furukawa, S., Nagamatsu, A., Nenoi, M., Fujimori, A., Kakinuma, S., Katsube, T., Wang, B., Tsuruoka, C., Shirai, T., Nakamura, A.J., Sakaue-Sawano, A., Miyawaki, A., Harada, H., Kobayashi, M., Kobayashi, J., Kunieda, T., Funayama, T., Suzuki, M., Miyamoto, T., Hidema, J., Yoshida, Y., Takahashi, A., 2020. Space radiation biology for "living in space". BioMed Res. Int. 2020, 4703286.

Geiger, H., 2014. HSC senescence upon irradiation. Blood 123, 3060–3061.

Gorissen, B., de Bruin, A., Miranda-Bedate, A., Korthagen, N., Wolschrijn, C., de Vries, T.J., van Weeren, R., Tryfonidou, M.A., 2018. Hypoxia negatively affects senescence in osteoclasts and delays osteoclastogenesis. J. Cell. Physiol. 234, 414–426.

Green, D.E., Adler, B.J., Chan, M.E., Rubin, C.T., 2012. Devastation of adult stem cell pools by irradiation precedes collapse of trabecular bone quality and quantity. J. Bone Miner. Res. 27, 749–759.

Greenberger, J.S., Epperly, M., 2009. Bone marrow-derived stem cells and radiation response. Semin. Radiat. Oncol. 19, 133–139.

Grigor'ev, A.I., Krasavin, E.A., Ostrovskiĭ, M.A., 2013. [Galactic heavy charged particles damaging effect on biological structures]. Ross Fiziol Zh Im I M Sechenova 99, 273–280.

Hamilton, S.A., Pecaut, M.J., Gridley, D.S., Travis, N.D., Bandstra, E.R., Willey, J.S., Nelson, G.A., Bateman, T.A., 2006. A murine model for bone loss from therapeutic and space-relevant sources of radiation. J. Appl. Physiol. 1985 (101), 789–793.

Kacena, M.A., Nelson, T., Clough, M.E., Lee, S.K., Lorenzo, J.A., Gundberg, C.M., Horowitz, M.C., 2006. Megakaryocyte-mediated inhibition of osteoclast development. Bone 39, 991–999.

Kelm, R.J., Hair, G.A., Mann, K.G., Grant, B.W., 1992. Characterization of human osteoblast and megakaryocyte-derived osteonectin (SPARC). Blood 80, 3112–3119.

Kennedy, A.R., 2014. Biological effects of space radiation and development of effective countermeasures. Life Sci. Space Res. 1, 10–43.

Lee, Y.S., Kwak, M.K., Moon, S.A., Choi, Y.J., Baek, J.E., Park, S.Y., Kim, B.J., Lee, S.H., Koh, J.M., 2020. Regulation of bone metabolism by megakaryocytes in a paracrine manner. Sci. Rep. 10, 2277.

Liu, F., Wang, Z., Li, W., Wei, Y., 2019. Transcriptional response of murine bone marrow cells to total-body carbon-ion irradiation. Mutat. Res. Genet. Toxicol. Environ. Mutagen 839, 49–58.

Macaulay, I.C., Thon, J.N., Tijssen, M.R., Steele, B.M., MacDonald, B.T., Meade, G., Burns, P., Rendon, A., Salunkhe, V., Murphy, R.P., Bennett, C., Watkins, N.A., He, X.,

Fitzgerald, D.J., Italiano, J.E., Maguire, P.B., 2013. Canonical Wnt signaling in megakaryocytes regulates proplatelet formation. Blood 121, 188–196.
Magrin, G., Mayer, R., Verona, C., Grevillot, L., 2015. Radiation quality and ion-beam therapy: understanding the users' needs. Radiat. Protect. Dosim. 166, 271–275.
Manolagas, S.C., Jilka, R.L., 1995. Bone marrow, cytokines, and bone remodeling. Emerging insights into the pathophysiology of osteoporosis. N. Engl. J. Med. 332, 305–311.
Mauch, P., Constine, L., Greenberger, J., Knospe, W., Sullivan, J., Liesveld, J.L., Deeg, H.J., 1995. Hematopoietic stem cell compartment: acute and late effects of radiation therapy and chemotherapy. Int. J. Radiat. Oncol. Biol. Phys. 31, 1319–1339.
Muralidharan, S., Sasi, S.P., Zuriaga, M.A., Hirschi, K.K., Porada, C.D., Coleman, M.A., Walsh, K.X., Yan, X., Goukassian, D.A., 2015. Ionizing particle radiation as a modulator of endogenous bone marrow cell reprogramming: implications for hematological cancers. Front. Oncol. 5, 231.
Nguyen, H.Q., To, N.H., Zadigue, P., Kerbrat, S., De La Taille, A., Le Gouvello, S., Belkacemi, Y., 2018. Ionizing radiation-induced cellular senescence promotes tissue fibrosis after radiotherapy. A review. Crit. Rev. Oncol. Hematol. 129, 13–26.
Norbury, J.W., Schimmerling, W., Slaba, T.C., Azzam, E.I., Badavi, F.F., Baiocco, G., Benton, E., Bindi, V., Blakely, E.A., Blattnig, S.R., Boothman, D.A., Borak, T.B., Britten, R.A., Curtis, S., Dingfelder, M., Durante, M., Dynan, W.S., Eisch, A.J., Robin Elgart, S., Goodhead, D.T., Guida, P.M., Heilbronn, L.H., Hellweg, C.E., Huff, J.L., Kronenberg, A., La Tessa, C., Lowenstein, D.I., Miller, J., Morita, T., Narici, L., Nelson, G.A., Norman, R.B., Ottolenghi, A., Patel, Z.S., Reitz, G., Rusek, A., Schreurs, A.S., Scott-Carnell, L.A., Semones, E., Shay, J.W., Shurshakov, V.A., Sihver, L., Simonsen, L.C., Story, M.D., Turker, M.S., Uchihori, Y., Williams, J., Zeitlin, C.J., 2016. Galactic cosmic ray simulation at the NASA space radiation laboratory. Life Sci. Space Res. 8, 38–51.
Pignolo, R.J., Law, S.F., Chandra, A., 2021. Bone aging, cellular senescence, and osteoporosis. JBMR Plus 5, e10488.
Rana, T., Schultz, M.A., Freeman, M.L., Biswas, S., 2012. Loss of Nrf2 accelerates ionizing radiation-induced bone loss by upregulating RANKL. Free Radic. Biol. Med. 53, 2298–2307.
Restier-Verlet, J., El-Nachef, L., Ferlazzo, M.L., Al-Choboq, J., Granzotto, A., Bouchet, A., Foray, N., 2021. Radiation on earth or in space: what does it change. Int. J. Mol. Sci. 22.
Richardson, R.B., 2009. Ionizing radiation and aging: rejuvenating an old idea. Aging (N Y) 1, 887–902.
Rithidech, K.N., Golightly, M., Whorton, E., 2008. Analysis of cell cycle in mouse bone marrow cells following acute in vivo exposure to 56Fe ions. J. Radiat. Res. 49, 437–443.
Schindelin, J., Arganda-Carreras, I., Frise, E., Kaynig, V., Longair, M., Pietzsch, T., Preibisch, S., Rueden, C., Saalfeld, S., Schmid, B., Tinevez, J.Y., White, D.J., Hartenstein, V., Eliceiri, K., Tomancak, P., Cardona, A., 2012. Fiji: an open-source platform for biological-image analysis. Nat. Methods 9, 676–682.
Schönmeyr, B.H., Wong, A.K., Soares, M., Fernandez, J., Clavin, N., Mehrara, B.J., 2008. Ionizing radiation of mesenchymal stem cells results in diminution of the precursor pool and limits potential for multilineage differentiation. Plast. Reconstr. Surg. 122, 64–76.
Shahnazari, M., Dwyer, D., Chu, V., Asuncion, F., Stolina, M., Ominsky, M., Kostenuik, P., Halloran, B., 2012. Bone turnover markers in peripheral blood and marrow plasma reflect trabecular bone loss but not endocortical expansion in aging mice. Bone 50, 628–637.
Shao, L., Luo, Y., Zhou, D., 2014. Hematopoietic stem cell injury induced by ionizing radiation. Antioxidants Redox Signal. 20, 1447–1462.
Sharaf-Eldin, W.E., Abu-Shahba, N., Mahmoud, M., El-Badri, N., 2016. The modulatory effects of mesenchymal stem cells on osteoclastogenesis. Stem Cell. Int. 2016, 1908365.
Singh, A.K., Althoff, M.J., Cancelas, J.A., 2018. Signaling pathways regulating hematopoietic stem cell and progenitor aging. Curr. Stem Cell Rep. 4, 166–181.
Stavnichuk, M., Mikolajewicz, N., Corlett, T., Morris, M., Komarova, S.V., 2020. A systematic review and meta-analysis of bone loss in space travelers. NPJ Micrograv. 6, 13.
Su, P., Tian, Y., Yang, C., Ma, X., Wang, X., Pei, J., Qian, A., 2018. Mesenchymal stem cell migration during bone formation and bone diseases therapy. Int. J. Mol. Sci. 19.
Suman, S., Maniar, M., Fornace, A.J., Datta, K., 2012. Administration of ON 01210.Na after exposure to ionizing radiation protects bone marrow cells by attenuating DNA damage response. Radiat. Oncol. 7, 6.
Teitelbaum, S.L., 2000. Bone resorption by osteoclasts. Science 289, 1504–1508.
Walker, S.A., Townsend, L.W., Norbury, J.W., 2013. Heavy ion contributions to organ dose equivalent for the 1977 galactic cosmic ray spectrum. Adv. Space Res. 51, 1792–1799.
Wang, Y., Chang, J., Li, X., Pathak, R., Sridharan, V., Jones, T., Mao, X.W., Nelson, G., Boerma, M., Hauer-Jensen, M., Zhou, D., Shao, L., 2017. Low doses of oxygen ion irradiation cause long-term damage to bone marrow hematopoietic progenitor and stem cells in mice. PLoS One 12, e0189466.
Wang, Y., Xu, L., Wang, J., Bai, J., Zhai, J., Zhu, G., 2021. Radiation induces primary osteocyte senescence phenotype and affects osteoclastogenesis in vitro. Int. J. Mol. Med. 47.
Willey, J.S., Lloyd, S.A., Nelson, G.A., Bateman, T.A., 2011a. Space radiation and bone loss. Gravit Space Biol. Bull. 25, 14–21.
Willey, J.S., Lloyd, S.A., Nelson, G.A., Bateman, T.A., 2011b. Ionizing radiation and bone loss: space exploration and clinical therapy applications. Clin. Rev. Bone Miner. Metabol. 9, 54–62.
Xiao, M., Wang, Y., Tao, C., Wang, Z., Yang, J., Chen, Z., Zou, Z., Li, M., Liu, A., Jia, C., Huang, B., Yan, B., Lai, P., Ding, C., Cai, D., Xiao, G., Jiang, Y., Bai, X., 2017. Osteoblasts support megakaryopoiesis through production of interleukin-9. Blood 129, 3196–3209.
Yang, B., Zhou, H., Zhang, X.D., Liu, Z., Fan, F.Y., Sun, Y.M., 2012. Effect of radiation on the expression of osteoclast marker genes in RAW264.7 cells. Mol. Med. Rep. 5, 955–958.
Yu, H., Shen, H., Yuan, Y., XuFeng, R., Hu, X., Garrison, S.P., Zhang, L., Yu, J., Zambetti, G.P., Cheng, T., 2010. Deletion of Puma protects hematopoietic stem cells and confers long-term survival in response to high-dose gamma-irradiation. Blood 115, 3472–3480.
Zhang, J., Wang, Z., Wu, A., Nie, J., Pei, H., Hu, W., Wang, B., Shang, P., Li, B., Zhou, G., 2017. Differences in responses to X-ray exposure between osteoclast and osteoblast cells. J. Radiat. Res. 58, 791–802.
Zhao, M., Perry, J.M., Marshall, H., Venkatraman, A., Qian, P., He, X.C., Ahamed, J., Li, L., 2014. Megakaryocytes maintain homeostatic quiescence and promote post-injury regeneration of hematopoietic stem cells. Nat. Med. 20, 1321–1326.